AIAA 81-1472R

Finite Element Solutions of Transonic Flow Problems

Wagdi G. Habashi*
Concordia University, Montreal, Canada
and
Mohamed M. Hafez*
George Washington University, Hampton, Virginia

The artificial compressibility method is briefly reviewed and the effect of different forms of the artificial viscosity are studied. Successful finite element solutions of transonic airfoil problems are presented. Iterative procedures including VLSOR, Zebroid, fast solver, first- and second-degree methods, and variable acceleration parameters such as preconditioned steepest descent and conjugate gradient are discussed and necessary modifications for transonic flow computations by finite elements are implemented leading to fast, reliable, and efficient calculations.

Introduction

THE analysis and design of modern transonic aircraft and turbomachinery requires efficient and accurate numerical solution algorithms. Transonic flows around airfoils, wings, and cascades have been successfully computed with iterative type-dependent finite differences, where accurate treatments of boundary conditions dictate the use of global transformations or mappings. For more complex configurations local transformations provided by isoparametric finite elements are attractive. Such an approach has been used by Jameson and Caughey[1] in their finite volume calculations. Direct applications of finite element techniques have been made by Glowinski et al.[2] based on an optimal control formulation.

More straightforward finite element calculations of transonic flows have been reported by Eberle,[3] using vertical line successive over-relaxation (VLSOR) and the artificial compressibility method (ACM), where the density is modified to introduce an artificial viscosity. The artificial compressibility method is now widely used in both finite difference and finite element calculations.[4-13]

In this paper, various forms of the artificial density are studied and several iterative algorithms are developed and tested. Numerical results are presented for both subsonic and supersonic freestream Mach numbers.

Governing Equation, Boundary Conditions, and Finite Element Representation

The transonic full potential equation, in conservation form, for two-dimensional flows is

$$\left(\frac{\rho}{\rho_0}\phi_x\right)_x+\left(\frac{\rho}{\rho_0}\phi_y\right)_y=0 \tag{1}$$

where

$$\frac{\rho}{\rho_0}=\left[1-\frac{\gamma-1}{2}\frac{(\nabla\phi)^2}{a_0^2}\right]^{1/(\gamma-1)} \tag{2}$$

together with the boundary conditions of surface impermeability, Kutta condition, and far-field behavior.

From Fig. 1a therefore,

$$\frac{\partial\phi}{\partial n}=0 \text{ on the body} \tag{3a}$$

$$\phi=V_\infty[x\cos\alpha+y\sin\alpha]; \quad x,y\to\infty \tag{3b}$$

For subsonic flows, Eq. (1) is elliptic and standard variational methods are applicable.[14] Finite difference, finite volume, and finite element discretization techniques can be developed and indeed the results of such calculations are generally in good agreement.

In this work we adopt the isoparametric quadrilateral bilinear element for which the function ϕ is represented as

$$\phi=\sum_{i=1}^{4}N_i\phi_i=\{N^{(e)}\}^T\{\phi\}^{(e)} \tag{4a}$$

$$N_i(\xi,\eta)=\tfrac{1}{4}(1+\xi\xi_i)(1+\eta\eta_i) \tag{4b}$$

where (ξ,η) are the natural coordinates of the undistorted element (Fig. 1b) and the superscript e refers to the element e.

The Galerkin weighted-residual method, applied to the operator of Eq. (1) requires

$$\iint_D RN_i\,dA=0 \tag{5}$$

where $R=L(\phi)$ is the residual and D represents the solution domain. Rewriting $L(\phi)$ explicitly and assuming (ρ/ρ_0) to be given by the previous iteration

$$\sum_{e=1}^{m}\iint N_i\left[\frac{\partial}{\partial x}\left(\frac{\rho}{\rho_0}\frac{\partial\phi^{(e)}}{\partial x}\right)+\frac{\partial}{\partial y}\left(\frac{\rho}{\rho_0}\frac{\partial\phi^{(e)}}{\partial y}\right)\right]dx\,dy=0 \tag{6}$$

Substituting Eq. (4) into Eq. (6), and integrating by parts yields

$$\{k\}^{(e)}\{\phi\}^{(e)}=\{f\}^{(e)}$$

where

$$k_{ij}^{(e)}=\left(\frac{\rho}{\rho_0}\right)^{(e)}\iint_{A^{(e)}}\left[\frac{\partial N_i}{\partial x}\frac{\partial N_j}{\partial x}+\frac{\partial N_i}{\partial y}\frac{\partial N_j}{\partial y}\right]dx\,dy$$

and

$$f^{(e)}=\oint_{C^{(e)}}N_i\left(\frac{\partial\phi}{\partial n}\right)ds \tag{7}$$

Presented as Paper 81-1472 at the AIAA/SAE/ASME 17th Joint Propulsion Conference, Colorado Springs, Colo., July 27-29, 1981; submitted Aug. 12, 1981; revision received Jan. 21, 1982.

*Associate Professor; also Consultant, Pratt & Whitney Aircraft of Canada Ltd., Longueuil, Canada. Member AIAA.

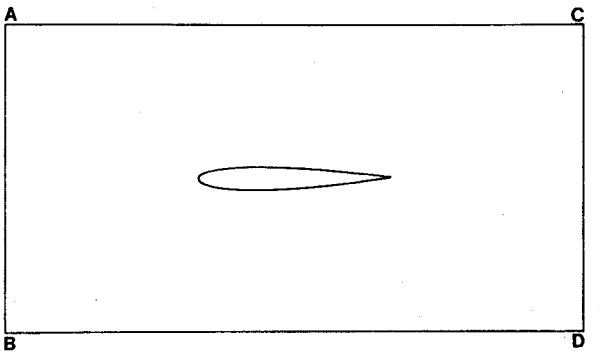

Fig. 1a Isolated airfoil computational domain.

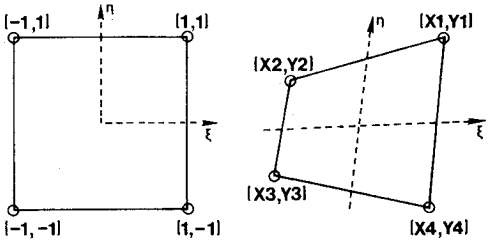

Fig. 1b Isoparametric bilinear element.

and f exists only for edges on the outer boundary of the domain over which $\partial\phi/\partial n$ does not vanish.

The isoparametric concept allows one to represent the geometry (x,y) with the same functional behavior representing (ϕ) itself, i.e.,

$$x=\sum_{i=1}^{4} N_i x_i; \quad y=\sum_{i=1}^{4} N_i y_i \tag{8}$$

Since the shape functions N_i of the element are written in terms of the natural local coordinates system (ξ,η), the terms $\partial N_i/\partial x$ and $\partial N_i/\partial y$ in Eq. (7) are obtained from

$$\begin{Bmatrix} \frac{\partial N_i}{\partial x} \\ \frac{\partial N_i}{\partial y} \end{Bmatrix} = \begin{bmatrix} \frac{\partial x}{\partial \xi} & \frac{\partial y}{\partial \xi} \\ \frac{\partial x}{\partial \eta} & \frac{\partial y}{\partial \eta} \end{bmatrix}^{-1} \begin{Bmatrix} \frac{\partial N_i}{\partial \xi} \\ \frac{\partial N_i}{\partial \eta} \end{Bmatrix} = |J|_i^{-1} \begin{Bmatrix} \frac{\partial N_i}{\partial \xi} \\ \frac{\partial N_i}{\partial \eta} \end{Bmatrix} \tag{9}$$

and the local element influence matrix can be rewritten as

$$k_{ij}^{(e)} = \left(\frac{\rho}{\rho_0}\right)^{(e)} \iint_{A^{(e)}} F(\xi,\eta)\,|J|^{(e)}\,d\xi d\eta \tag{10}$$

and can be evaluated via 2×2 numerical Gaussian integration.

After performing the assembly for all elements, one obtains

$$[K]\{\phi\}=\{F\} \tag{11}$$

Dissipative Discretizations

The above discretization is not dissipative. As the freestream Mach number increases a supersonic bubble appears and Eq. (1) becomes locally hyperbolic and the solution may be discontinuous. To capture these details, an artificial viscosity is needed.

One way of introducing the required artificial viscosity in the supersonic region is to use upwind differencing. Special switching operators are then needed to obtain conservative solutions, due to the mixed-type nature of the transonic equation.[15] The finite element analog of upwind differencing has recently been studied for convection dominated flows[16] and is complicated. For application to transonic flows, special blending elements would be needed across the sonic line and the shock wave, as discussed by Hafez et al.[17] and Guderley.[18]

Alternatively, the artificial viscosity terms, in conservation form, can be explicitly added and the modified equation is discretized using standard finite difference methods. For example, Jameson[19] solved

$$(\rho u+P)_x+(\rho v+Q)_y=0 \tag{12}$$

where

$$P=-\mu u\rho_x\Delta x, \quad Q=-\mu v\rho_y\Delta y, \quad \mu=\max[0,1-(1/M^2)] \tag{13}$$

Δx, Δy = grid spacing in x, y directions. The P and Q terms are approximations of the artificial viscosity term introduced by the upwind differencing used in Jameson's earlier non-conservative calculations. Combining Eqs. (12) and (13), and recasting in terms of the velocity potential leads to the form

$$(\rho_1\phi_x)_x+(\rho_2\phi_y)_y=0 \tag{14}$$

where

$$\rho_1=\rho-\mu\rho_x\Delta x, \quad \rho_2=\rho-\mu\rho_y\Delta y$$

A slightly different artificial viscosity leads to the simpler form suggested by Hafez et al.[4]

$$(\tilde{\rho}\phi_x)_x+(\tilde{\rho}\phi_y)_y=0 \tag{15}$$

where

$$\tilde{\rho}=\rho-\mu\rho_s\Delta s, \quad \rho_s\Delta s=(u/q)\rho_x\Delta x+(v/q)\rho_y\Delta y, \quad q^2=u^2+v^2$$

The artificial compressibility method can be based on either Eq. (14) or Eq. (15), the latter being adopted in this work.

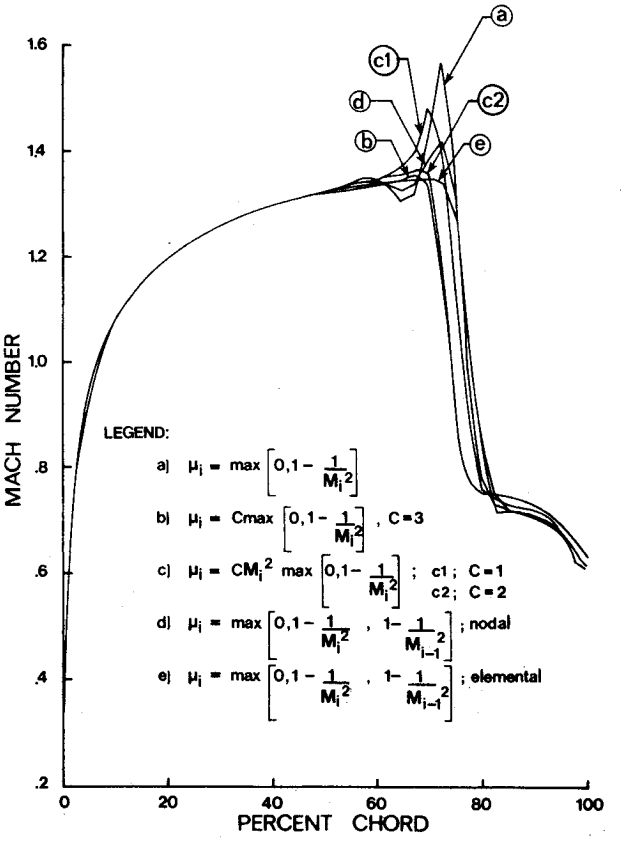

Fig. 2 Comparison of switching functions.

In all published finite element results based on the artificial compressibility method,[20] the switching function μ has been amplified by a factor ranging from M^2 to $2M^2$, otherwise a peaky solution is obtained at the shock. It seems that this higher viscosity is indispensable for the stability of these calculations and consequently shocks are weakened and displaced upstream when compared with published finite difference calculations that use lower artificial viscosity.

In order to avoid the need for this excessive artificial viscosity, we propose modifying the switching operator as follows

$$\mu = \max[0,\ \mu_i,\ \mu_{i-1}] \tag{16}$$

where

i = nodal point at which equation is applied
$i-1$ = point directly upstream of i
$\mu_i = 1 - (1/M_i^2)$

Both finite difference and finite element results based on Eq. (16) have proved free of peaks, while shocks are not smeared out. In Fig. 2 we demonstrate the effect of various switching functions on the finite element solution of the flow around a NACA 0012 airfoil at $M_\infty = 0.85$. Result (a) demonstrates the need for an enhanced artificial viscosity at the shock while results (b) and (c1, c2) show the detrimental effect of introducing more dissipation. In cases (d) and (e) we demonstrate the advantages of Eq. (16).

In Fig. 3 we obtain the inviscid limit of our solution by solving the above-mentioned test case for three equally spaced values of $1/\mu$ and nonlinearly extrapolating the three results to the inviscid limit ($1/\mu \to \infty$).

In Fig. 4 the results of calculations based on a constant artificial viscosity are shown. It should be mentioned that the calculations with constant viscosity are about 25% faster than using variable viscosity, at the cost of smearing the shock.

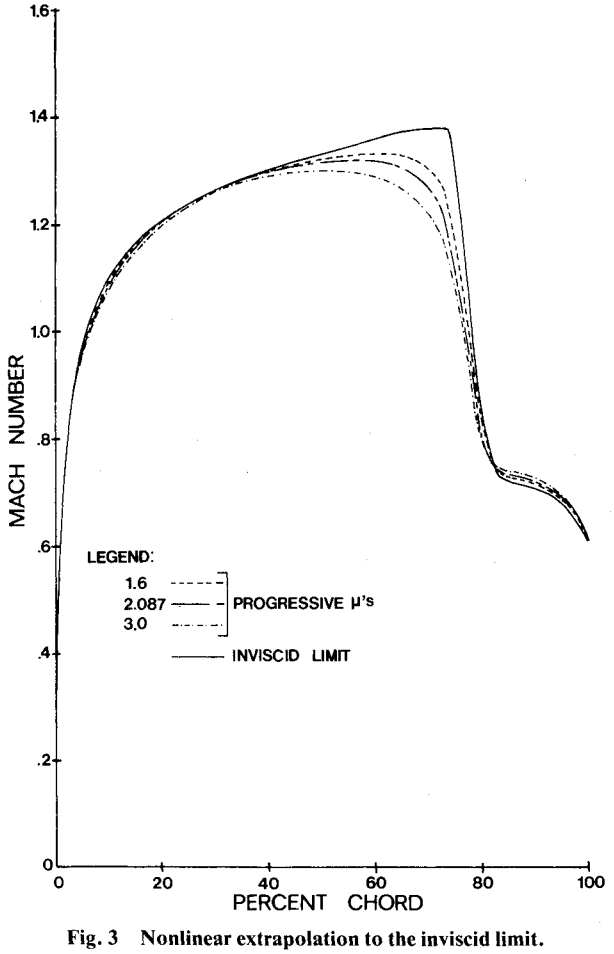

Fig. 3 Nonlinear extrapolation to the inviscid limit.

Figure 5 shows our results for $M_\infty = 0.72$, 0.85, and 0.95 over a NACA 0012 airfoil. In particular our method has no difficulty capturing the details of the fishtail shock at $M_\infty = 0.95$. In addition the figure presents the results for a supersonic inlet Mach number of 1.2 and shows the details of the bow shock and the oblique shock at the trailing edge.

Comparisons with other published finite element results are given in Figs. 6-8. The differences, sometimes rather large, are attributed to the effect of the lower artificial viscosity used here and the manner in which it is implemented.

Figure 9 shows the development of the solution through iteration for the field solvers proposed in this paper and Fig. 10 shows the Mach number contours for freestream Mach numbers of 0.85 and 0.95. The grid used is a curvilinear, unequally spaced (70×15) grid, with 45 points on the airfoil and inlet/exit conditions imposed 3 chords upstream/downstream.

In the next section, the convergence of iteration is discussed and the various iterative algorithms used in this work are detailed.

Iterative Procedures

In the past, attempts to solve Eq. (14) or (15) by finite elements using elliptic methods have failed for high Mach numbers. In such methods the density is assumed to be known from a previous iteration and the equations always look elliptic, $\tilde{\rho}$, ρ_1, and ρ_2 being positive for both subsonic and supersonic regions. Such a linearization, however, is inconsistent and bound to lead to convergence difficulties since the nonlinearity is essential and responsible for the mixed-type nature of the equation.

In the following, different iterative algorithms for transonic flow calculations are discussed.

Vertical Line Successive Over-relaxation (VLSOR)

Most finite difference calculations are based on VLSOR. The finite element calculations of Eberle[3] are also based on VLSOR. Marching with the flow, the development of the

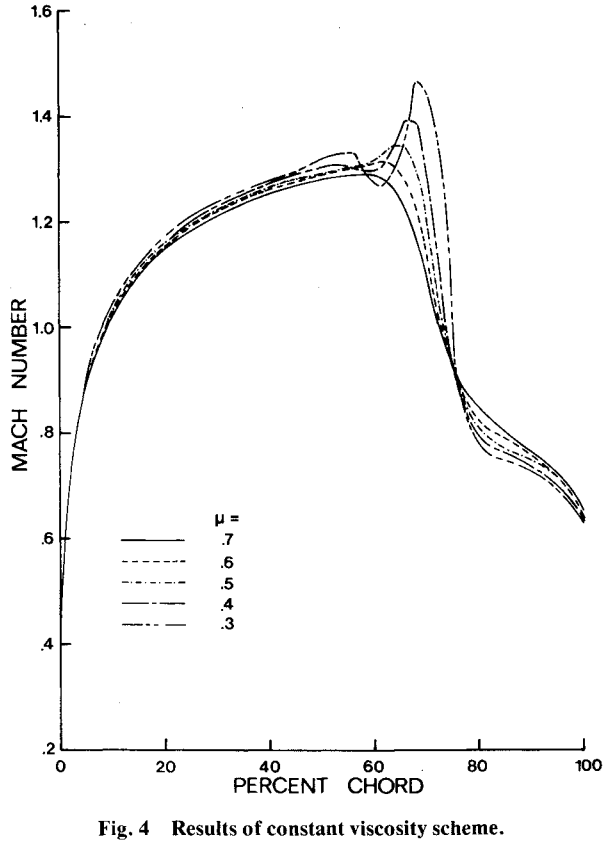

Fig. 4 Results of constant viscosity scheme.

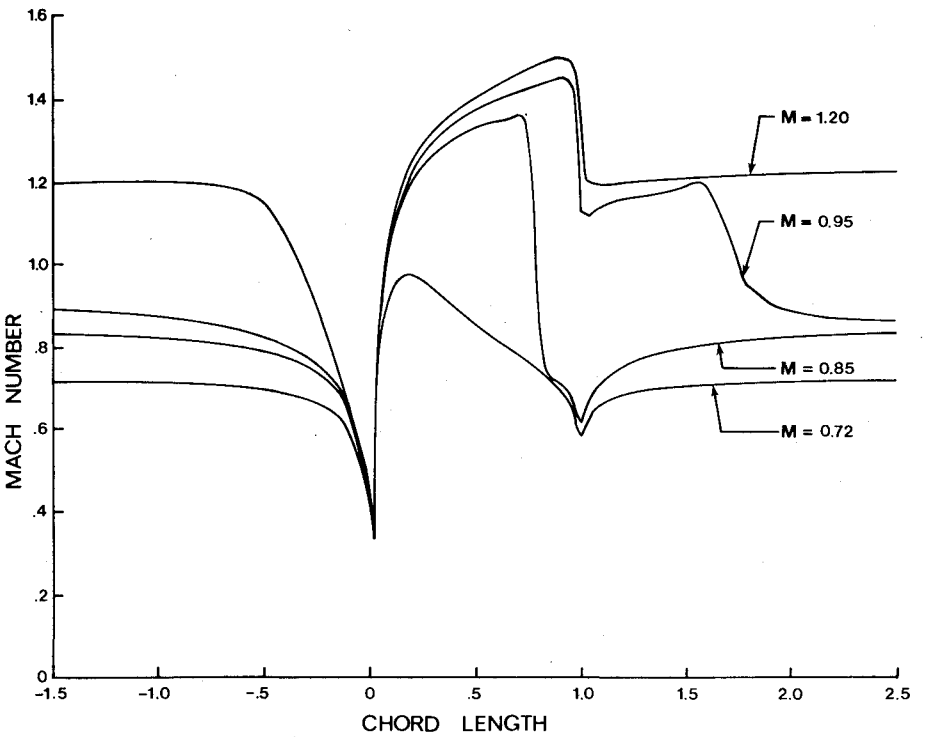

Fig. 5 Present finite element method results (NACA 0012) for a range of Mach numbers.

solution with iteration can be described by an artificial time-dependent equation which is a damped hyperbolic equation for subsonic points. For supersonic points, x is the time-like direction and errors are propagated rather than damped.

The VLSOR algorithm for finite differences can be recast in the form[4]

$$\alpha\phi_t + \beta\phi_{xt} + \gamma\phi_{yyt} = R \tag{17}$$

where R is the residual.

It is found that convergence is improved for transonic cases if the coefficient of the ϕ_{xt} term is explicitly augmented. Such a term is added directly to the VLSOR algorithm at each station during iteration.

Similarly for finite element calculations, it is found that an augmented ϕ_{xt} term is needed, otherwise calculations diverge for high Mach numbers, as illustrated in Fig. 11. The figure shows convergence of the $\|L\|_2^2$ residual, R_{L-2}, against iterations, where

$$\|L\|_2 = \sqrt{\sum_{i=1}^{n} R_i^2}$$

Zebroid Scheme

For subsonic flows, successive horizontal line over-relaxation is an alternative, with a ϕ_{yt} term in the modified equation. The sign of this term depends on the marching direction. Such a scheme does not converge for higher Mach numbers. If, however, odd and even lines are alternately updated, no ϕ_{yt} term is produced. A $\phi_{xt}(\phi_{st})$ term is then explicitly added leading to fast convergence for transonic calculations.[21]

Results for $M_\infty = 0.72$, 0.85, 0.95, and 1.2 based on the Zebroid scheme are shown in Fig. 12.

Fast Solver

For moderate transonic cases, the following iterative procedure is used

$$A\delta\phi = -\omega R^n \tag{18}$$

where A is the Laplacian incompressible operator and ω a relaxation factor.

For high Mach numbers, the above procedure does not converge. Jameson[19] suggested to alternate between the VLSOR and fast solvers and obtained a rapid rate of convergence.

Similarly, for finite element calculations reported here, an LL^T decomposition of the Laplacian (incompressible) operator $(\partial_{xx} + \partial_{yy})$ is alternated with the VLSOR algorithm augmented by ϕ_{xt}.

At the high Mach numbers, say $M_\infty = 0.95$, it is found that a fixed number of VLSOR sweeps between fast solvers may not lead to a convergent process. We found the best criterion was to carry out a minimum number of intermediate VLSOR sweeps (say 10) but only go back to the field solver if the VLSOR residual has decreased below the last field solver solution residual.

First- and Second-Degree Iterative Methods

Two- and three-level schemes can be written in the form

$$A\delta\phi = -\beta R \quad \text{for two-level schemes} \tag{19a}$$

$$A\delta^2\phi + \alpha A\delta\phi = -\beta R \quad \text{for three-level schemes} \tag{19b}$$

where α and β are fixed acceleration parameters, and A is an asymmetric operator constructed by modifying the stiffness matrix k_{ij} of each element as follows:

$$[k_{ij}^*] = [k_{ij}][T_{ij}] \tag{20}$$

where T_{ij} is an element transformation matrix reducing the contribution at a supersonic point, say s (Fig. 13), from downstream nodes (D1, D2, D3) within the elements (E1, E2), while enhancing the contribution to that point from the upstream nodes (U1, U2, U3) in elements on its left (E3, E4).

The method bears a similarity to schemes used by Chan and Brashears[22] and Marsh and Eastep.[23] In effect it is simple to show that such a transformation induces a ϕ_{xt} term in the artificial time-dependent equation describing the development

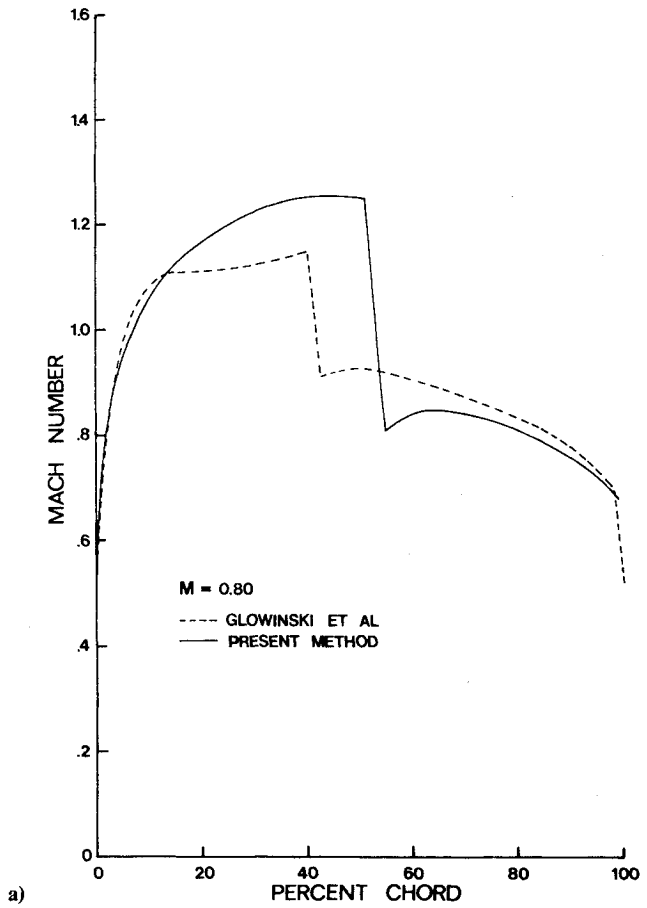

a)

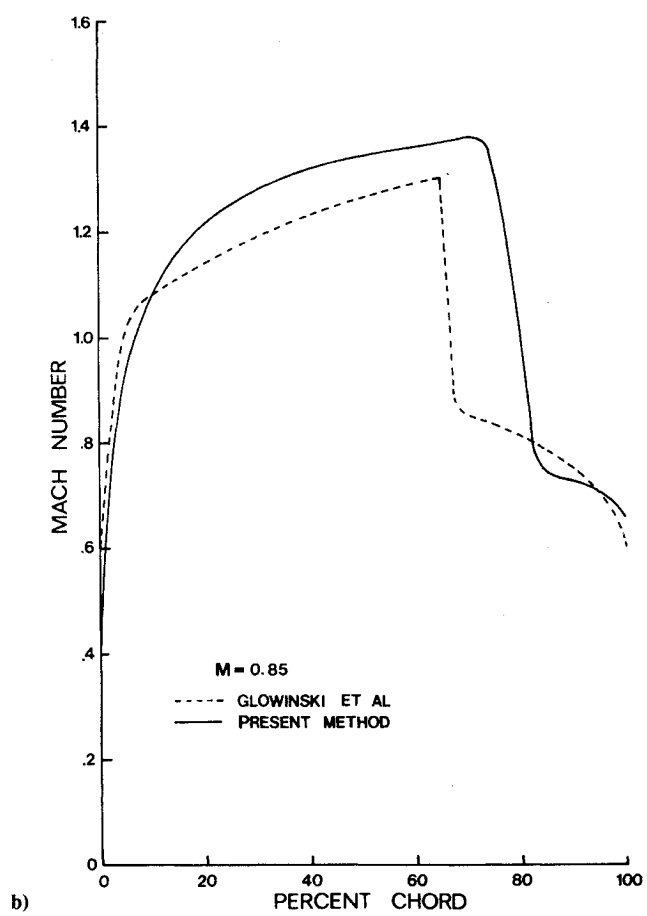

b)

Fig. 6 NACA 0012 FEM comparison against Ref. 2.

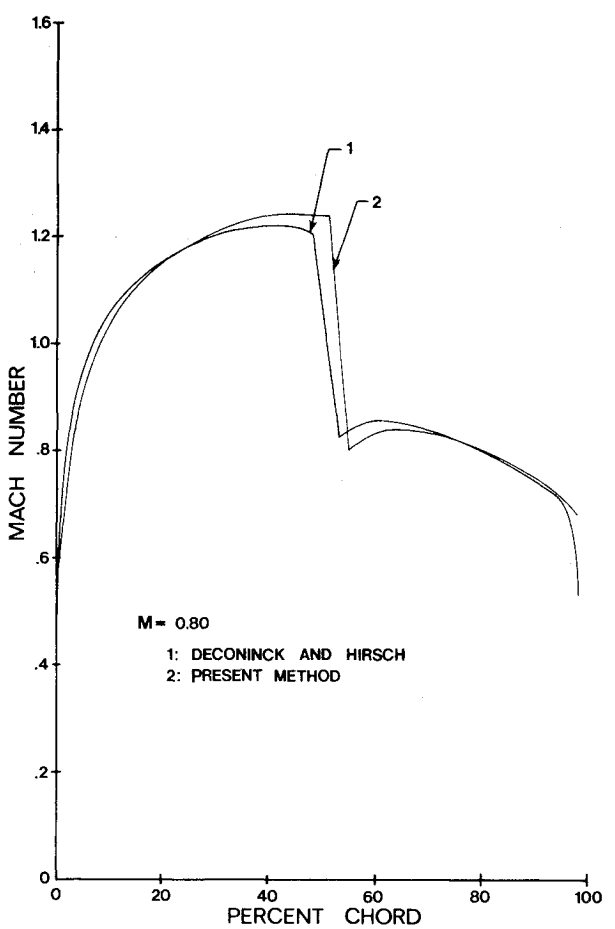

a)

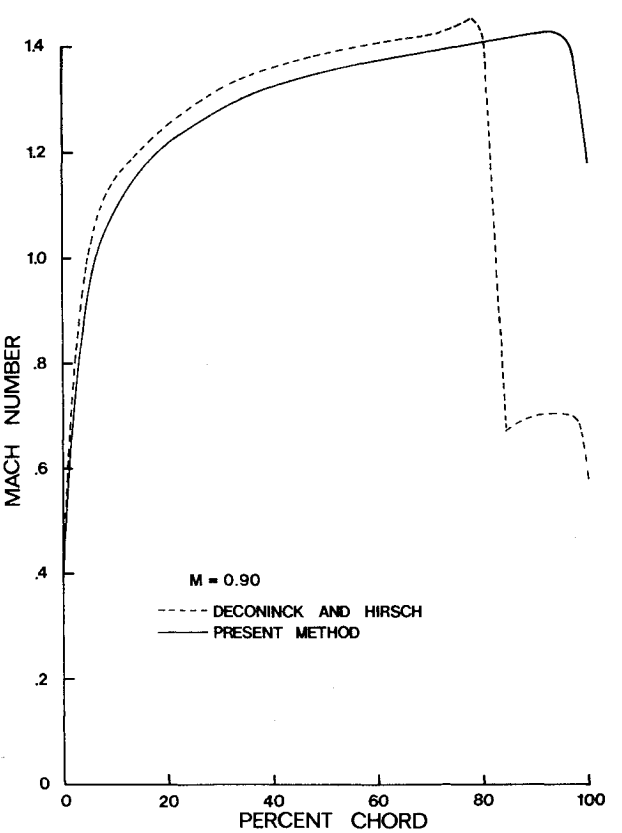

b)

Fig. 7 NACA 0012 FEM comparison against Ref. 6.

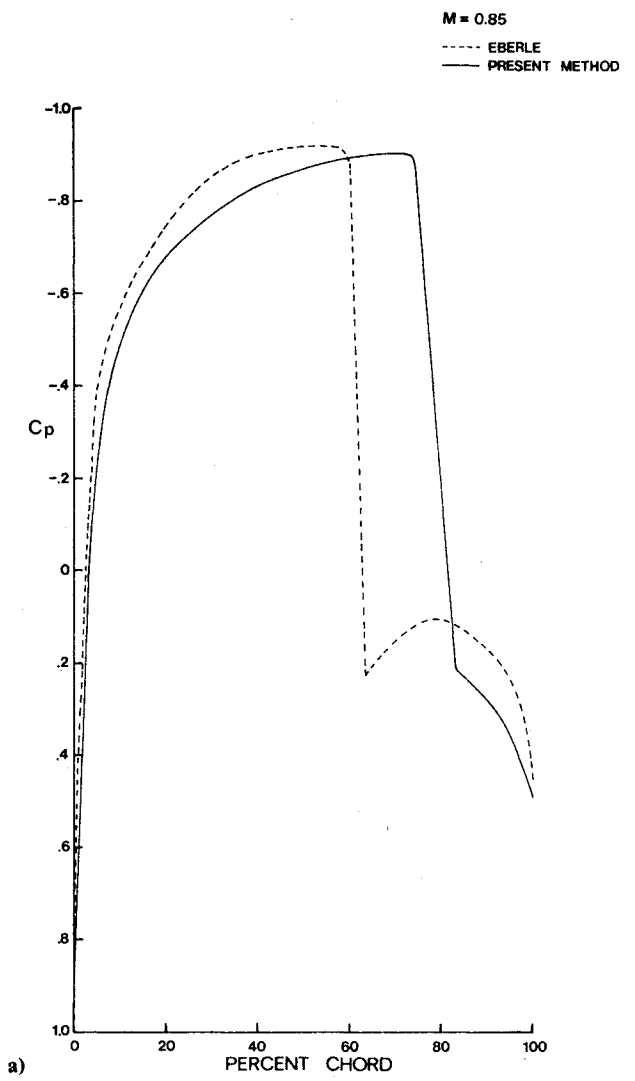

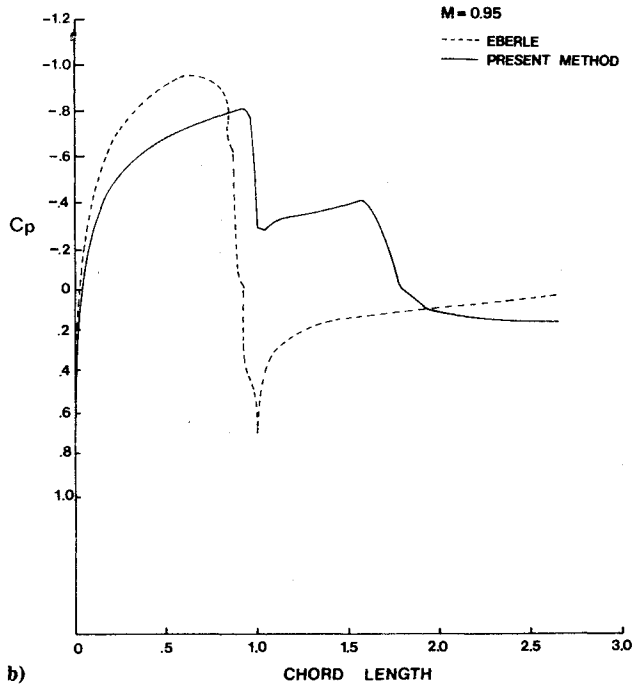

Fig. 8 NACA 0012 FEM comparison against Ref. 20.

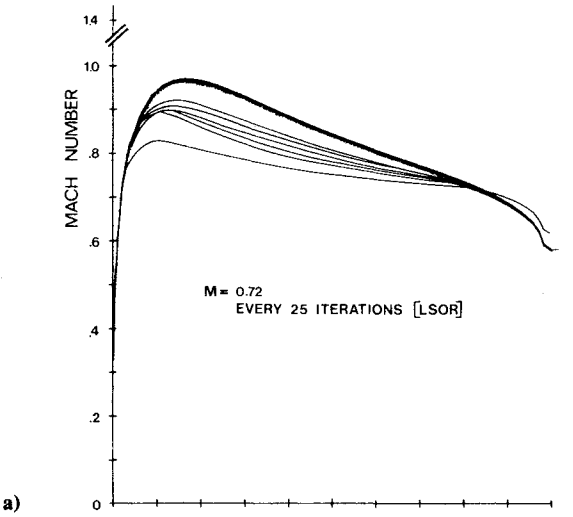

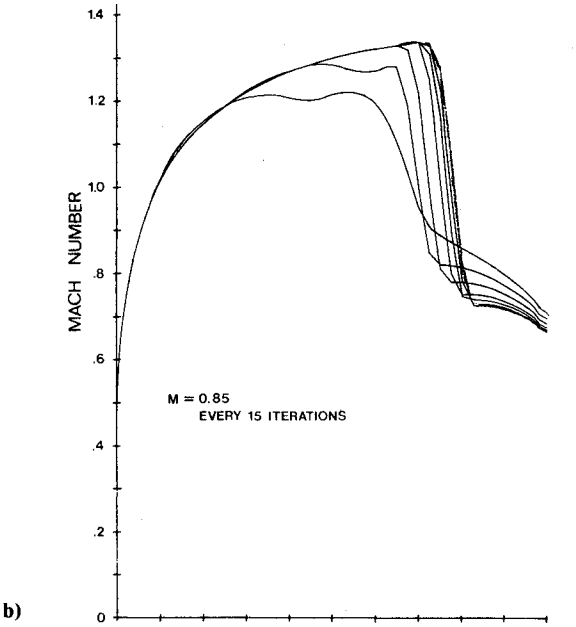

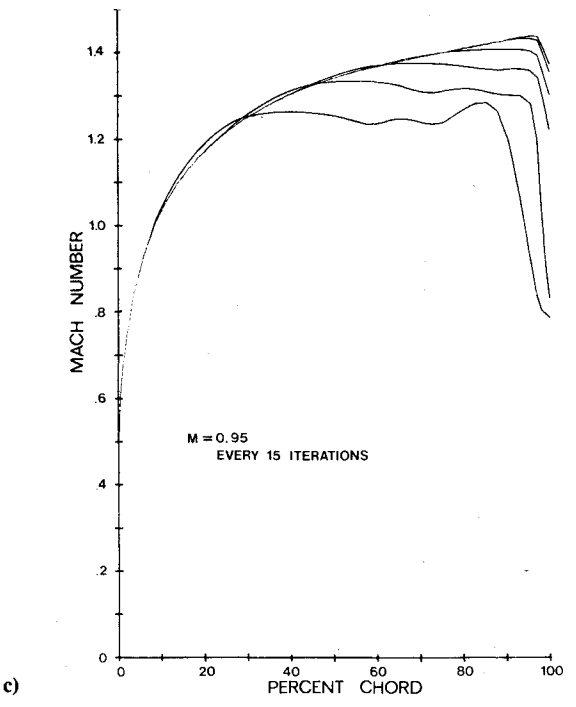

Fig. 9 Solution development with iteration, NACA 0012: a) VLSOR solver; b) Φ_t solver; c) Φ_t solver.

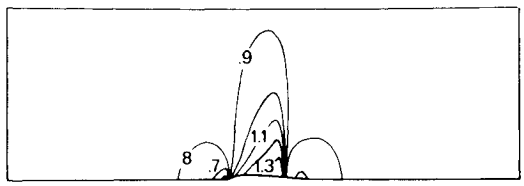

Fig. 10a Mach number contours for NACA 0012 at $M = 0.85$.

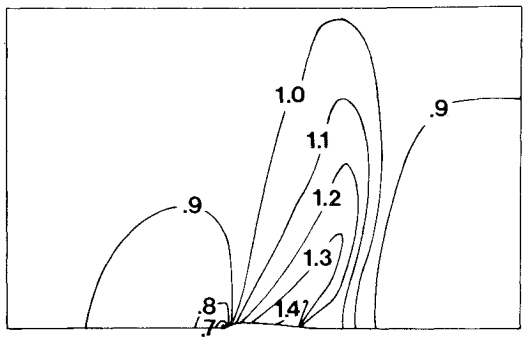

Fig. 10b Mach number contours for NACA 0012 at $M = 0.95$.

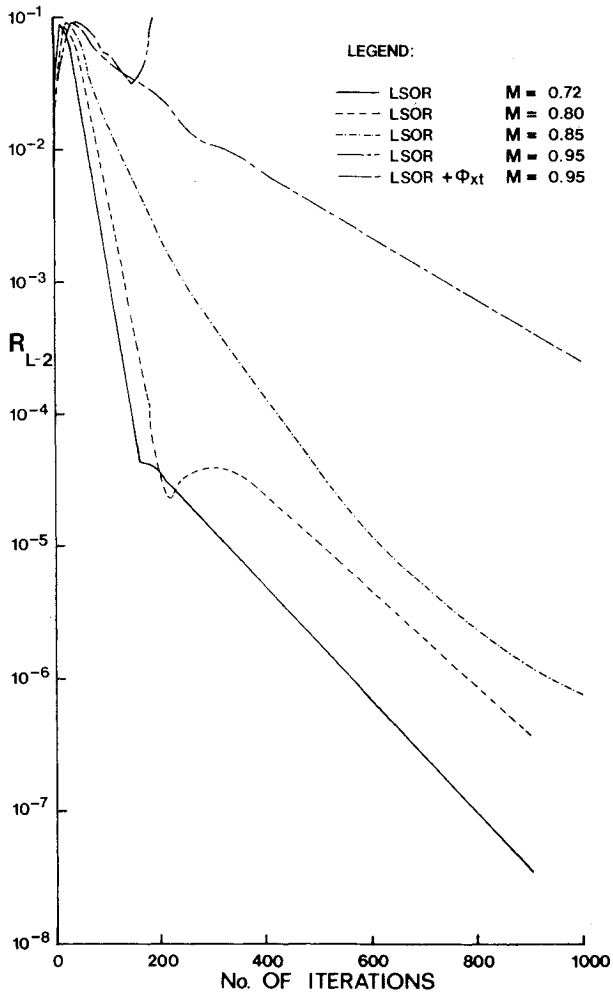

Fig. 11 Rate of convergence of VLSOR algorithm.

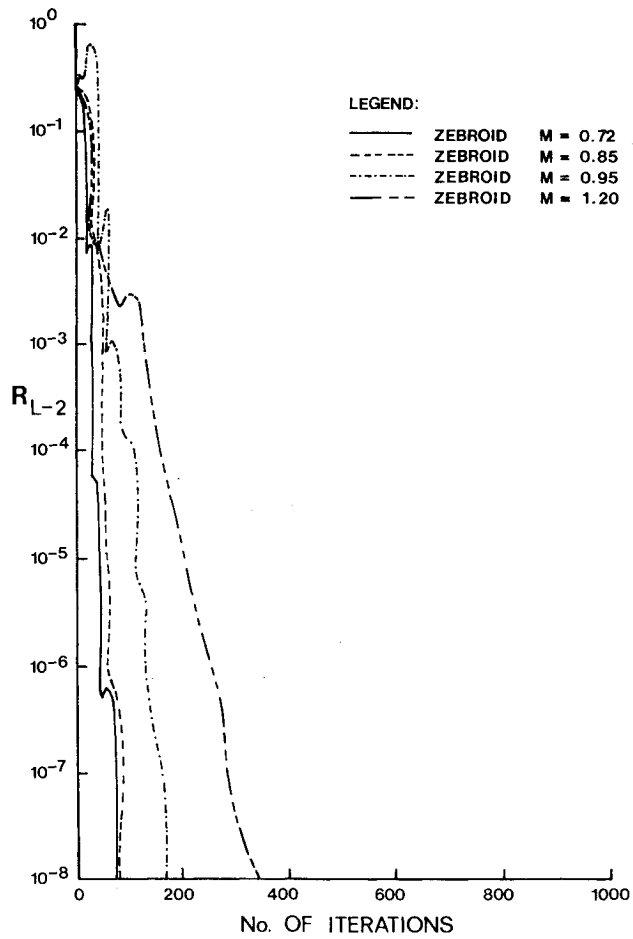

Fig. 12 Rate of convergence of Zebroid algorithm.

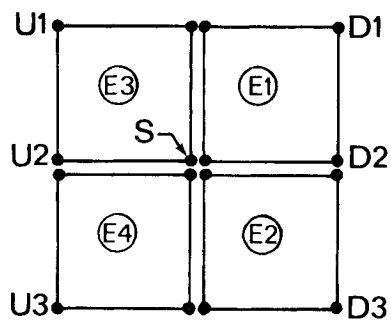

Fig. 13 Introducing the Φ_{xt} term in the Φ_t solver.

of the solution through iteration and hence guarantees stability at the high Mach numbers.

An exact LU decomposition of the asymmetric operator is used first. An efficient approximate LU factorization (incomplete decomposition), where the zero pattern of the matrix is preserved, has also been successfully tested. Results are shown in Fig. 14.

The incomplete decomposition saves 40% of the calculation per iteration and does not affect the rate of convergence at transonic speeds. A further saving is obtained by updating the density less frequently, as often as each eight iterations. It should be mentioned that the elemental formulation consisting of assuming the density to be constant in each element and calculating it at the centroid is much faster than the nodal formulation of calculating the density at the four corners of the elements meeting at a node and averaging to obtain a nodal value.

Successive mesh refinement techniques have been tested but the savings were pronounced only for subcritical flows.

To avoid repeated exact or approximate decomposition of the asymmetric matrix, a Laplacian is used in Eq. (19) and the above procedure is alternated with a VLSOR containing an

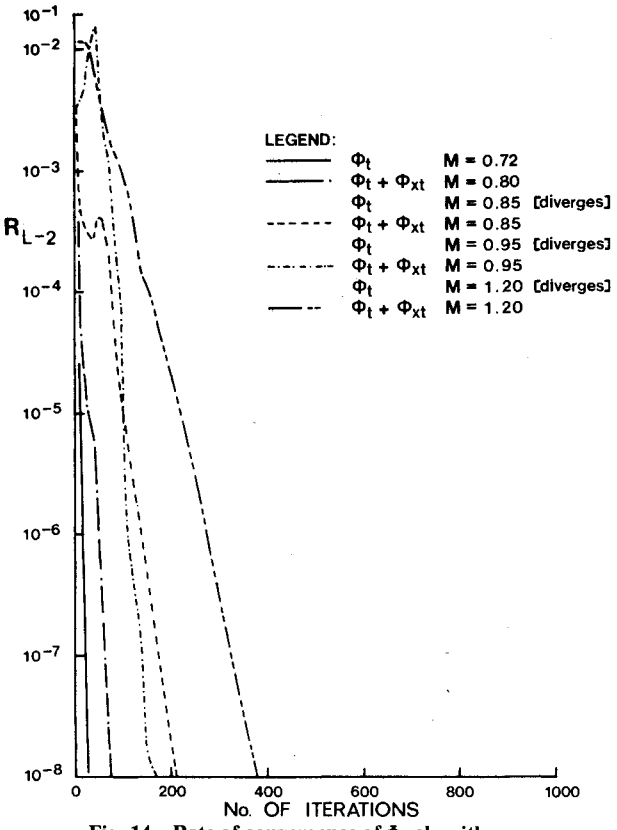

Fig. 14 Rate of convergence of Φ_t algorithm.

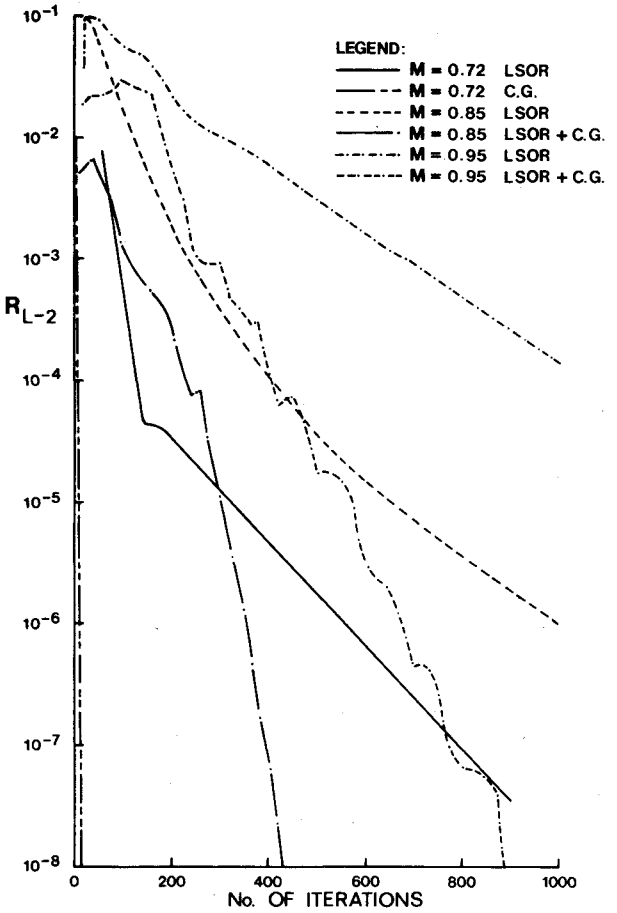

Fig. 15 Rate of convergence of preconditioned gradient methods.

enhanced ϕ_{xt} term. Another way to produce a ϕ_{xt} effect is to modify the density by a ϕ_t term, as discussed by Hafez et al.[4] The artificial density becomes

$$\frac{\tilde{\rho}}{\rho_0} = \left[1 - \frac{\gamma - 1}{2} \frac{(\nabla\phi)^2 + \mu\phi_t}{a_0^2}\right]^{1/(\gamma-1)} \tag{21}$$

where $\mu = \max[0, 1 - (1/M^2)]$ or one could simply use

$$\tilde{\rho} = \rho - \mu(\rho_s \Delta s + \alpha\phi_t) \tag{22}$$

It should be mentioned that the ϕ_{xt} term produced in this manner is lagged iterationwise and hence may not be as effective as alternating with VLSOR. Satisfactory results have been obtained for low transonic Mach numbers.

Variable Acceleration Parameters: Preconditioned Gradient Methods

Variable acceleration parameters, based on preconditioned conjugate gradient methods,[24] have also been tested as shown in Fig. 15.

Four algorithms have been tested: preconditioned conjugate gradient, steepest descent, minimum residual method, and minimum residual on the correction. Such schemes worked very efficiently for subsonic and mildly transonic cases, converging for example in 14 iterations for NACA 0012 at $M_\infty = 0.72$ to a residual $R_{L-2} = 10^{-8}$. At the higher Mach number, say $M_\infty = 0.85$, convergent iteration was achieved when intermediate VLSOR sweeps were used to produce enough ϕ_{xt} to stabilize the algorithm, leading to much faster convergence than VLSOR alone. Such methods are being further investigated. They hold promise for three-dimensional flows as well.

Conclusions

The finite element method has been applied to transonic flow using a variety of iterative techniques. Most published finite element calculations have used excessive artificial viscosity, otherwise peaks occur upstream of the shocks.[20] In this work, a simple modification of the switching operator in the artificial compressibility method is introduced and good results, free of peaks, are obtained with a lower artificial viscosity. Results based on a constant artificial viscosity everywhere and an inviscid limit obtained by nonlinear extrapolation are also promising.

Line relaxation methods calculations based on VLSOR are painfully slow. However, the Zebroid scheme has proved to be fast and reliable. First- and second-degree iterative methods with ϕ_{xt} terms and an incomplete decomposition method remain a viable alternative. The same can be said about conjugate gradient methods coupled with a VLSOR solver.

All results presented here are for isolated airfoils; application to turbomachinery will be reported elsewhere.[25]

Acknowledgment

The authors would like to thank Peter Kotiuga and Vish Bhat of Pratt & Whitney Aircraft for their programming assistance. This research was partially supported by Contract PRAI-7901 and Grant A-3662 of the Natural Sciences and Engineering Council of Canada (NSERC).

References

[1] Jameson, A. and Caughey, D. A., "Finite Volume Method for Transonic Full Potential Calculations," *Proceedings of AIAA Third Computational Fluid Dynamics Conference*, June 1977, AIAA, New York, 1977, pp. 33-54.

[2] Glowinski, R. and Pironneau, O., "On the Computation of Transonic Flows," Paper presented at France/Japanese Conference on Functional Analysis and Numerical Analysis, Tokyo/Kyoto, Sept. 1976.

[3] Eberle, A., "Transonic Potential Flow Computations by Finite Element: Airfoil and Wing Analysis, Airfoil Optimization," MBB-UFE 1428 ö-DGLR 78-65, 1978.

[4] Hafez, M., South, J., and Murman, E., "Artificial Compressibility Methods for Numerical Solutions of Transonic Full Potential Equation," *AIAA Journal*, Vol. 17, Aug. 1979, pp. 838-844.

[5] Holst, T. L., "An Implicit Algorithm for the Conservation Transonic Full Potential Equation Using an Arbitrary Mesh," *AIAA Journal*, Vol. 17, Oct. 1979, pp. 1038-1045.

[6] Deconinck, H. and Hirsch, Ch., "Finite Element Methods for Transonic Blade-to-Blade Calculation in Turbomachines," *ASME Journal of Engineering for Power*, Vol. 103, Oct. 1981, pp. 665-677.

[7] Caspar, J. R., "A Mode Problem Study of Transonic Potential Flow Procedures," AIAA Paper 80-0337, Jan. 1980.

[8] Habashi, W. G. and Kotiuga, P. L., "Numerical Solution of Transonic Cascade Flows," Paper presented at the ASME Century 2 Emerging Technologies Conference and Aerospace Conference, San Francisco, Aug. 1980.

[9] Yu, N. J. and Rubbert, P. E., "Acceleration Schemes for Transonic Potential Flow Calculations," AIAA Paper 80-0338, Jan. 1980.

[10] Farrell, C. and Adamczyk, J., "Full Potential Solution of Transonic Quasi-3-D Flow Through a Cascade Using Artificial Compressibility," Paper 81-GT-70, presented at ASME International Gas Turbine Conference, Houston, Texas, March 1981.

[11] Akay, H. U. and Ecer, A., "Transonic Flow Computations in Cascades Using Finite Element Method," *ASME Journal of Engineering for Power*, Vol. 103, Oct. 1981, pp. 657-664.

[12] Sankar, N. L., Malone, J. B., and Tassa, Y., "An Implicit Conservative Algorithm for Steady and Unsteady Three Dimensional Transonic Potential Flows," *AIAA 5th Computational Fluid Dynamics Conference Proceedings*, AIAA, New York, 1981.

[13] Wong, Y. S. and Hafez, M. M., "Preconditioned Conjugate Gradient Methods for Transonic Flow Calculations," *Preconditioning Techniques for the Numerical Solution of P.D.E.*, edited by D. J. Evans (to appear).

[14] Shen, S. F. and Habashi, W. G., "Local Linearization of the Finite Element Method and Its Applications to Compressible Flows," *International Journal for Numerical Methods in Engineering*, Vol. 10, 1976, pp. 565-577.

[15] Murman, E. M., "Analysis of Embedded Shock Calculated by Relaxation Methods," *AIAA Journal*, Vol. 12, May 1974, pp. 626-633.

[16] Hughes, T.J.R., Ed., *Finite Element Methods for Convection Dominated Flows*, ASME AMD, Vol. 34, 1979.

[17] Hafez, M. M., Wellford, L. C., Merkle, C. L., and Murman, E. M., "Numerical Computation of Transonic Flows by Finite Element and Finite Difference Methods," NASA-CR-3070, Dec. 1978.

[18] Guderley, K. G., "The Treatment of the Sonic Line and of Shocks in a Finite Element Approach to Transonic Flow Computations," AFWAL TR-80-3046, June 1980.

[19] Jameson, A., "Transonic Flow Calculation," VKI Lecture Series 87, March 1976.

[20] Rizzi, A. and Viviand, H., Eds., *Notes on Numerical Fluid Mechanics, GAMM Workshop on Numerical Methods for the Computation of Inviscid Transonic Flows with Shock Waves*, Vieweg & Sohn, 1980.

[21] Hafez, M. M. and South, J. C., "Vectorization of Relaxation Methods for Solving Transonic Full Potential Equation," GAMM Workshop on Numerical Methods for the Computation of Inviscid Transonic Flow with Shock Waves, FAA Stockholm, Sweden, Sept. 1979.

[22] Chan, S. T. and Brashears, M. R., "Analysis of Steady and Unsteady Transonic Flows by Finite Element Method," AFFDL-TR-75-11, March 1974.

[23] Marsh, J. E. and Eastep, F. E., "Analysis of a Symmetric Transonic Airfoil with the Finite Element Method—A New Technique," *International Journal for Numerical Methods in Engineering*, Vol. 16, 1980, pp. 137-148.

[24] Wong, Y. S. and Hafez, M. M., "Application of Conjugate Gradient Methods to Transonic Finite Difference and Finite Element Calculations," *Proceedings of AIAA 5th Computational Fluid Dynamics Conference*, Palo Alto, June 1981, pp. 272-283.

[25] Habashi, W. G. and Kotiuga, P. L., "Finite Element Solution of Subsonic and Transonic Cascade Flows," *Proceedings of the Second International Conference on Numerical Methods in Laminar and Turbulent Flow*, Venice, Italy, July 1981, pp. 1253-1265, also, *International Journal for Numerical Methods in Fluids*, in press.